ACS APPLIED MATERIALS & INTERFACES
Research Article
www.acsami.org

Flame-Retardant Paper from Wood Fibers Functionalized via Layer-by-Layer Assembly

Oruç Köklükaya,*[†] Federico Carosio,[‡] Jaime C. Grunlan,[§] and Lars Wågberg*[†,∥]

[†]Fiber and Polymer Technology, KTH Royal Institute of Technology, Teknikringen 56, 100 44 Stockholm, Sweden
[‡]Dipartimento di Scienza Applicata e Tecnologia, Politecnico di Torino, Alessandria Site Viale Teresa Michel 5, 15121, Alessandria, Italy
[§]Department of Mechanical Engineering, Texas A&M University, College Station, Texas 77843, United States
[∥]Wallenberg Wood Science Center, KTH Royal Institute of Technology, SE-100 44 Stockholm, Sweden

S *Supporting Information*

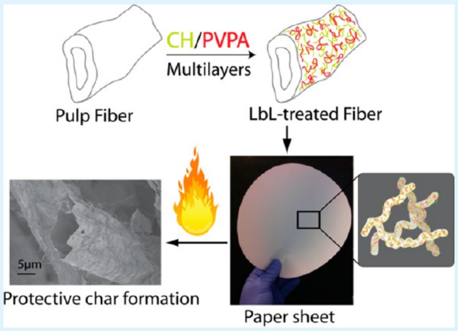

ABSTRACT: The highly flammable character of cellulose-rich fibers from wood limits their use in some advanced materials. To suppress the flammability and introduce flame-retardant properties to individual pulp fibers, we deposited nanometer thin films consisting of cationic chitosan (CH) and anionic poly(vinylphosphonic acid) (PVPA) on fibers using the layer-by-layer (LbL) technique. The buildup of the multilayer film was investigated in the presence and absence of salt (NaCl) using model cellulose surfaces and a quartz crystal microbalance technique. Fibers were then treated with the same strategy, and the treated fibers were used to prepare paper sheets. A horizontal flame test (HFT) and cone calorimetry were conducted to evaluate the combustion behavior of paper sheets as a function of the number of bilayers deposited on fibers. In HFT, paper made of fibers coated with 20 CH/PVPA bilayers (BL), self-extinguished the flame, while uncoated fibers were completely consumed. Scanning electron microscopy of charred paper after HFT revealed that a thin shell of the charred polymeric multilayer remained after the cellulose fibers had been completely oxidized. Cone calorimetry demonstrated that the phosphorus-containing thin films (20 BL is ∼25 nm) reduced the peak heat release rate by 49%. This study identifies a unique and highly effective way to impart flame-retardant characteristic to pulp fibers and the papers made from these fibers.

KEYWORDS: *layer-by-layer assembly, flame-retardant, thermal stability, wood fibers, chitosan, poly(vinylphosphonic acid)*

INTRODUCTION

A growing environmental concern and the depletion of petroleum resources have increasingly drawn attention to the need for alternatives to oil-based products by using natural and renewable resources. Cellulose obtained from wood and cotton is our most abundant natural polymer.[1] Wood-based cellulose has been the primary raw material for the pulp and paper industry for more than a century. Paper can be described as a three-dimensional fibrous network formed from a dilute water suspension of pulp fibers, and it is considered to be a biodegradable, recyclable, and inexpensive material. It is for these reasons that paper and fibrous networks have been used in many application areas such as corrugated fiber board, packaging materials, printing substrates, cleaning and hygiene products, and as insulation in, for example, high-voltage transformers.[2] Despite their many advantages, the highly flammable character of cellulosic fibers is a significant drawback that limits their application and many studies have focused on improving the flame-retardant behavior of cotton and cellulosic materials.[3] Paper-based products show reduced flammability after the incorporation of flame-retardant additives into the bulk of the fiber wall, either during the paper making process or as a post treatment of the paper. The most widely used additives contain elements such as phosphorus, halogens, and boron, or inorganic compounds such as silicates, hydroxides, and hydro-talcites.[4−6] Halogenated flame-retardants are the most commonly used and most effective, but studies have shown them to be persistent, bioaccumulative, and environmentally toxic for animals and humans.[7,8]

In recent years, layer-by-layer (LbL) assembly of polyelectrolytes and/or nanoparticles has been proposed as an alternative and eco-friendly flame-retardant treatment for several substrates such as cotton,[9−11] polyurethane foam,[12] plastic thin films[13,14] and PET fabrics.[15,16] LbL self-assembly was first presented by Iler in 1966 for microparticles[17] and gained more attention after its rediscovery and extensive development toward polyelectrolytes by Decher et al.[18] in the early 1990s. It consists of a multistep deposition process capable of forming multilayered thin films of oppositely charged polyelectrolytes and/or nanoparticles on nearly any solid

Received: August 31, 2015
Accepted: October 12, 2015
Published: October 12, 2015

DOI: 10.1021/acsami.5b08105
ACS Appl. Mater. Interfaces 2015, 7, 23750−23759

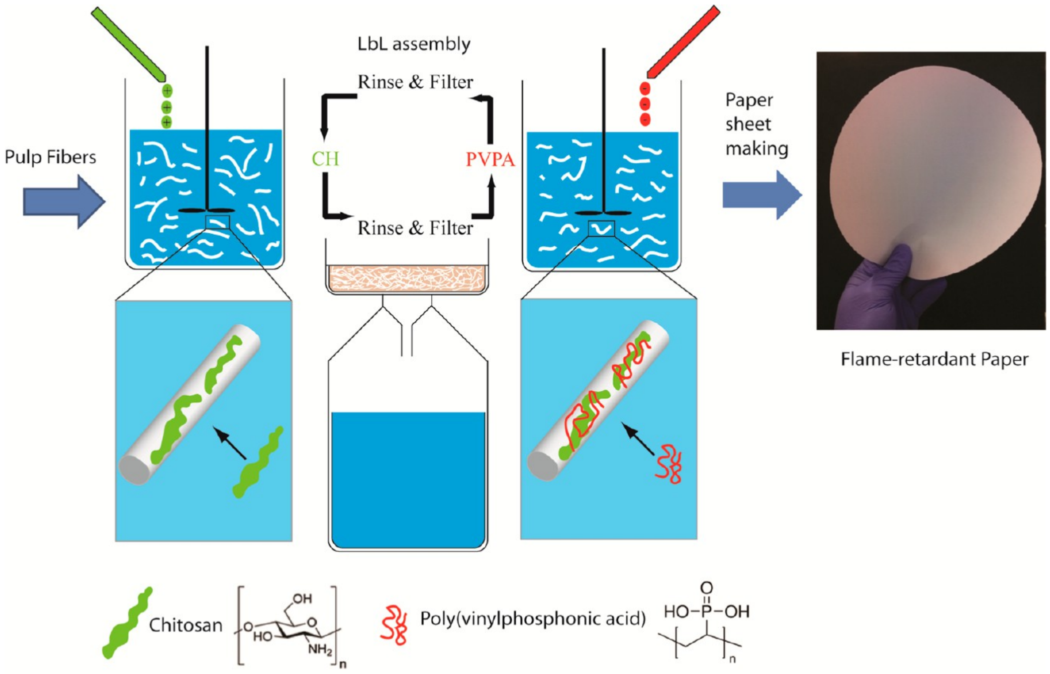

Figure 1. Schematic representation of layer-by-layer assembly of chitosan and poly(vinylphosphonic acid) onto pulp fibers, with washing and filtration between each deposition (one cycle deposits one bilayer). After the desired numbers of bilayers have been deposited, paper sheets can be prepared with the LbL-treated pulp fibers, as shown in the image (right).

surface.[19] This entropy-driven process has been used to form thin films mainly from electrostatically charged polymers/nanoparticles,[20] but a variety of other interactions have been exploited such as donor/acceptor,[21] hydrogen bonds,[22] and covalent bonds.[23] Thin films are most commonly built up on a selected substrate through sequential dipping[24] or spraying.[25] Moreover, the properties of LbL assemblies based on electrostatic attraction can be tuned by altering the chemistry of the polyelectrolyte,[26] polymer molecular weight,[27] temperature,[28] counterions,[29] ionic strength,[30] and pH of the solution.[31] In addition, the LbL technique offers several advantages such as multifunctionality of the deposited coatings, ambient application conditions and an eco-friendly nature due to the use of low (typically ≤1 wt %) concentration aqueous solutions or suspensions. In addition to flame-retardant characteristics,[10,11] the layer-by-layer self-assembly technique has been used to impart gas barrier,[32] antibacterial,[33] antireflection,[34] and electrical conductivity to a variety of solid surfaces.[35]

As far as flame retardancy is concerned, it is possible to target different surface flame-retardant mechanisms by the appropriate choice of the layer constituents and the deposition parameters. One of the most promising mechanisms is intumescence, a chemical process activated in the condensed phase (typically within a few microns of the surface) by flame or heat radiation. Due to the increase in temperature, the decomposition of a substance on the surface, typically a polymer, produces a swollen carbonaceous char layer that thermally insulates the underlying substrate and limits the release of flammable volatiles and oxygen transfer between the gas and condensed phases, resulting in a flame-retardant effect.[36] The LbL technique has been exploited in an effort to design intumescent nanocoatings by simultaneously providing the three ingredients needed for intumescence (i.e., a carbon source, an acid source, and a blowing agent). Li et al. have demonstrated the first intumescent coating on cotton,[37] and Carosio et al. have investigated an intumescent LbL assembly on polyester-cotton blends.[15] Laufer et al. have studied more eco-friendly LbL intumescent nanocoatings on cotton using renewable molecules.[38]

Wood fiber surfaces have also been exploited for LbL deposition to impart functionalities such as hydrophobicity, conductivity and improved mechanical properties of networks formed from the treated fibers.[39−41] The mechanical properties of paper materials prepared from LbL-treated pulp fibers are greatly improved due to the enhanced adhesion between the fibers.[40,42,43] In the present work, the LbL assembly technique has been employed for the first time to deposit chitosan (CH) and poly(vinylphosphonic acid) (PVPA) onto pulp fibers in an attempt to improve the flame-retardant properties of paper. A schematic representation of the deposition process used in this work is presented in Figure 1. The deposited bilayers of CH/PVPA provide an intumescent system in which CH[38,44] acts as both carbon source and blowing agent and PVPA can generate in situ phosphoric acid at elevated temperatures and act as the acid source.[45] The LbL model experiments were performed with silicon oxide surfaces and well-defined model cellulose surfaces and the thin film formation was studied as a function of layer number and electrolyte concentration. The most promising deposition conditions were then used to coat pulp fibers that were subsequently used for the preparation of paper sheets, as shown in Figure 1. The flame-retardant properties achieved were assessed by horizontal flame testing and cone calorimetry. The results showed that the flammability and combustibility of the sheets were significantly reduced.

■ EXPERIMENTAL SECTION

Materials. Fibers used were from a kraft soft wood pulp with average dimensions of 2 mm length, 20 μm diameter, and 4 μm fiber wall thickness, provided by SCA Forest Products (Östrand Pulp Mill), Sundsvall, Sweden, bleached with a chlorine-free (TCF) bleaching sequence: (OO)Q(OP) (ZQ) (PO), where O stands for oxygen, Q stands for chelating agent, P stands for hydrogen peroxide, and Z stands for ozone. The pulp was supplied as dry sheets that were disintegrated according to ISO 5263:1995 in deionized water. The pulp was washed, and the carboxyl groups present on fibers were converted to their sodium form according to a previously described procedure.[46] The surface charge of the fibers was found by the polyelectrolyte adsorption technique[47] to be 7.9 μequiv/g and the total charge by conductometric titration[48] to be 74 μequiv/g.

Chitosan (CH) with a molecular weight of 60 000 Da (according to the supplier) and 95% deacetylation was purchased from G.T.C Union Corporation (Qingdao, China). Poly(vinylphosphonic acid) (PVPA) with a molecular weight of 24 000 Da (according to the supplier) was purchased from Polysciences, Inc. (Eppelheim, Germany). CH was delivered as a powder and PVPA as a 30% aqueous solution. All chemicals were used as received without further purification. Cationic chitosan solutions were prepared by adjusting the pH of Milli-Q water to 2 with hydrochloric acid (HCl, 6 M), after which 0.1 wt % chitosan was added and the solution was magnetically stirred and left for 24 h to ensure complete dissolution. PVPA was diluted to a 0.1 wt % solution using 18.2 MΩ Milli-Q water. Both solutions pH was adjusted to 4 with sodium hydroxide (NaOH, 1M) prior the deposition. Polyvinylamine (PVAm) with a molecular weight of 45 000 Da, used as the anchoring layer for model cellulose surfaces, was supplied by BASF (Ludwigshafen, Germany). PVAm was dialyzed prior to 0.1 wt % solution preparation, the solution pH was adjusted to 7.5 prior to deposition. NaCl, HCl, and NaOH were all of analytical grade.

Polyelectrolyte Multilayers on Model Surfaces. Model cellulose surfaces were prepared according to a procedure described by Gunnars et al.[49] The fibers were dissolved and the solution spin-coated on a QCM quartz crystal with a 50 nm thick SiO_2 layer (QSX303) that had been saturated with a molecular layer of polyvinylamine (PVAm). PVAm was used as an anchoring layer on silicon wafer in order to enhance the homogeneous cellulose film formation. This procedure produces cellulose films with a thickness about 30 nm.[49] The consecutive deposition of CH and PVPA on this model cellulose surface was monitored with QCM-D (Qsense AB, Västra Frölunda, Sweden) following a procedure earlier described.[50] QCM has been described by Rodahl et al.[51] and it was here used to monitor the real time adsorption kinetics of the polyelectrolytes. The change in oscillating crystal frequency (Δf) is proportional to adsorbed mass, and the mass deposited was calculated using the Sauerbrey equation:[52]

$$\Delta m = C\frac{\Delta f}{n} \tag{1}$$

where m is adsorbed mass per area (mg m^{-2}), C is the sensitivity constant, −0,177 (mg m^{-2} Hz^{1-}), Δf is the change in oscillation frequency of the crystal (Hz) and n is the overtone number. The results from the third, fifth, and seventh overtones are shown in the present work. By measuring the decay in the oscillations with time after the driving current has been disconnected, it was also possible to determine the energy dissipation of the adsorbed layer and hence to collect information on the viscoelastic properties of the adsorbed layer.

The dry thickness of the multilayer thin films (1, 5, 10, and 20 BL) deposited on silica substrate was determined using an ellipsometer (Rudolph Research, Fairfiled, NJ) equipped with a mercury lamp and a filter for determination of an optical wavelength at 546.1 nm. A Nanoscope IIIa AFM, (Bruker AXS, Santa Barbara, CA) equipped with an E type piezoelectric scanner was used to image the surface morphology of the CH/PVPA films and determine the dry thickness by scratch height analysis. The silicon cantilever with a spring constant of 5 N/m (TAP 150, Bruker, Camarillo, CA) was used for tapping mode imaging in air. The thickness of the film was determined using step command in the AFM software, Nanoscope analysis.

Determination of Polyelectrolyte Adsorption onto Fibers. The polyelectrolyte adsorption isotherms for CH and PVPA on pulp fibers were determined by polyelectrolyte titration.[47] The adsorption time for chitosan was set to 30 min, and the CH remaining in solution was determined via back-titration of the filtrate with potassium polyvinylsulfate (KPVS), similar to that described by Terayama et al.,[53] with different initial chitosan concentrations. The adsorption saturation was calculated by extrapolating the isotherm to zero equilibrium concentration.[47] The surface charge of the pulp fibers was determined by polyelectrolyte titration following the adsorption of high molecular weight polydiallyldimethylammonium chloride (PDADMAC), which is not able to penetrate through the nanoporous fiber wall, and the surface charge was calculated from the adsorbed amount at saturation adsorption.[47]

For LbL formation on fibers, the fibers were treated alternately with cationic chitosan (CH) and anionic poly(vinylphosphonic acid) (PVPA). For each adsorption step, a fiber suspension with a background electrolyte concentration of 10 mM NaCl at pH 4 was prepared. The fibers were treated by adding 10 mg polyelectrolyte/g fiber for 10 min at room temperature. Between each treatment step, the fibers were washed twice using deionized water with the same electrolyte concentration (10 mM NaCl) and the same pH as the polyelectrolyte solutions (pH 4) (Figure 1). Excess rinsing water was removed using vacuum filtration. Polyelectrolyte titration was performed on the filtrates to determine the amount of polyelectrolyte adsorbed. Chitosan was titrated with analytical grade potassium polyvinylsulfate (KPVS) from Wako Pure Chemicals, Japan, while poly(vinylphosphonic acid) was titrated with polydiallyldimethylammonium chloride (PDADMAC), supplied by Sigma-Aldrich (Stockholm, Sweden).

Hand Sheet Preparation. Sheets made from CH/PVPA-treated fibers were used to investigate the influence of the adsorbed polymers on the flame retardant properties of paper. Sheets were prepared according to ISO 5269-2:1998, from a fiber dispersion (3.6 g/L) with a Rapid Köthen sheet former from PTI, Vorchdorf, Austria. The sheets were pressed at 95 kPa and dried at 93 °C for 15 min. In accordance with ISO 187:1990, paper sheets were conditioned at 23 °C and 50% relative humidity prior to testing. The target grammage of the sheets was 120 g/m^2, and the exact value was determined according to ISO 536:1995, and the thickness and density according to ISO 534:1998.

Thermal and Flame-Retardant Analysis. Thermal and thermo-oxidative degradation of wood fibers were investigated by thermogravimetric analysis (TGA) under nitrogen and air, respectively, (60 mL/min) from 50 to 800 °C, with a heating rate of 10 °C/min. Thermal analyses were conducted with ∼10 mg samples in open alumina pans, using a TA Instruments Q500 instrument, Laboratory for Emerging Material and Technology, South Carolina.

The flame-retardant behavior of the paper sheets were evaluated using the horizontal flame test (ASTM D 4986) with samples (30 × 100 mm) on a horizontal metallic frame. The samples were ignited on the short side by a 20 mm methane flame for 3 s. The test was repeated three times. The burning time, after-glow time, and amount of residue were determined. SEM images from some of the tested samples were also collected and analyzed.

The combustion of sheets made from untreated and LbL-treated fibers (100 × 100 mm) were investigated under irradiative heat flux (35 kW/m^2) using cone calorimetry (Fire Testing Technology, FTT, West Sussex, United Kingdom), following the procedure described elsewhere.[54] Time to ignition (TTI, s), heat release rate (HRR, kW/m^2), peak heat release rate (pkHRR, kW/m^2), total heat release (THR, kW/m^2) and final residue were measured.

The surface morphology of paper sheets prepared with untreated and LbL-treated fibers was investigated before and after the flammability test using a Hitachi S-4800 field emission scanning electron microscope (FE-SEM) to obtain secondary electron images. Test pieces from the sheets were fixed to conductive adhesive tape and coated with 5 nm thick platinum/palladium layer using a Cressington 208 HR High Resolution Sputter Coater.

RESULTS

Film Growth. Chitosan was selected as the cationic part and PVPA as the anionic component of this LbL system. PVPA shows excellent solution properties over a wide pH-range. It has

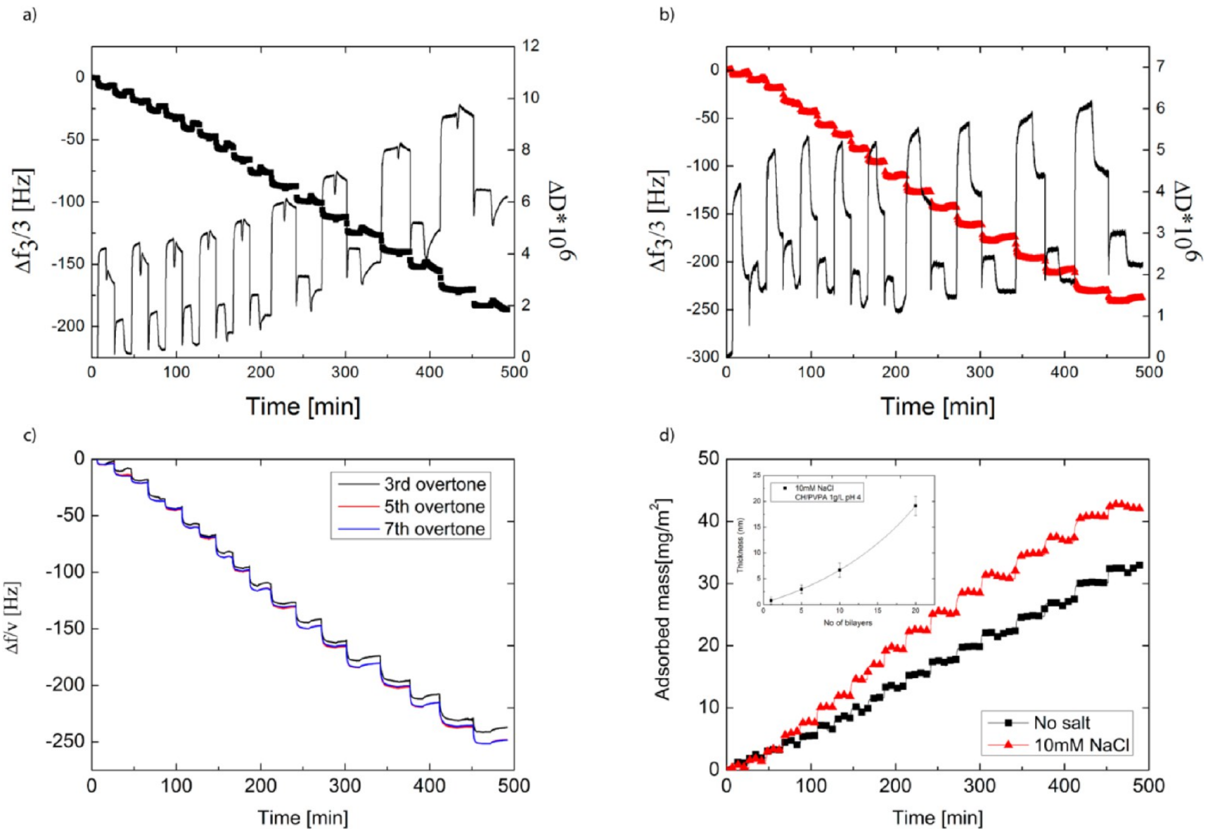

Figure 2. QCM-D normalized frequency shift and energy dissipation change for the third overtone upon LbL buildup of $(CH/PVPA)_9$ on a model cellulose surface (a) without salt and (b) with 10 mM NaCl; (c) the change in normalized frequency as a function of LbL formation for the third, fifth, and seventh overtone for the situation with added salt; and (d) the adsorbed mass including immobilized solvent calculated using the Sauerbrey equation for the third overtone with and without added salt. The CH and PVPA concentrations were kept constant at 1 g/L and the pH was constant at pH 4. (Inset) Thickness as a function of the number of bilayers deposited (CH/PVPA) on silica wafers measured using ellipsometry.

previously been shown[12,38] that it is necessary to keep the pH below 6.5 to achieve good solubility of the chitosan (pK_a 6−6.5), so the LbL formation was conducted at pH 4 in this study. This pH was also maintained for the PVPA adsorption and rinsing stages to ensure a good stability of the chitosan. The ionic strength was kept constant at 10 mM NaCl to achieve a high adsorption of polyelectrolytes in each adsorption step. The use of an acidic pH is not ideal for the adsorption of cationic polyelectrolytes onto cellulose but it was a compromise in the present system to ensure a good solubility and adsorption of the chitosan which is favorable for char formation.[12,38,55]

The multilayer thin film on the model cellulose surfaces[49] was characterized using QCM-D. Figure 2 shows the normalized frequency shift and the change in energy dissipation for the third overtone for assemblies of cationic chitosan and anionic poly(vinylphosphonic acid) with and without 10 mM NaCl as a background electrolyte concentration. The decrease in frequency is caused by the adsorbed polyelectrolyte and immobilized solvent in the adsorbed layer, while the dissipation provides information on the viscoelastic behavior of the thin film. Figure 2 shows a relatively low decrease in frequency with increasing number of bilayers regardless of ionic strength. The development of the dissipation is similar to that described earlier for the buildup of polyallyalmine hydrochloride (PAH) and poly(acrylic acid) (PAA) on SiO_2 surfaces,[56] and the odd−even effect of the dissipation is similar to that of the PAH/PAA system where a higher dissipation is achieved when the cationic polyelectrolyte is in the external layer. Figure 2c summarizes the change in normalized frequency for the experiments with added salt for three different overtones (third, fifth, and seventh overtone). The close similarity between the curves indicates the buildup of a rather homogeneous LbL structure. Figure 2d summarizes the adsorbed amount calculated with the Sauerbrey equation for the third overtone (eq 1) where both the solid amount of polymer and immobilized solvent are included. There is a significant increase in adsorbed amount with increasing ionic strength and these latter deposition conditions were therefore selected for further characterization and assembly onto cellulose fibers.

Morphology of Coated Surfaces. The surface morphology, thickness and roughness of the LbL assembled thin films were characterized using tapping mode AFM images, as shown for the CH/PVPA pair with different numbers of bilayers (1, 5, 10, and 20 BL) in Figure 3a−c. The thickness of the film at 20 BL was also determined by scanning the area scratched with a needle to remove a section of the LbL (Figure 3d). The height (Figure 3a) and phase (Figure 3b) images of CH/PVPA on silica surfaces show an uneven film formation in the early bilayers. The surface appears to be rough, on a nm level, and discontinuous for the first bilayers, with an average roughness value (rms-value) of 6.8 nm at 5 BL. When the BL number was increased to 10 and 20, the film became smoother with a continuous character and the rms value for the 20 BL film decreased to 2 nm. This is consistent with previously published

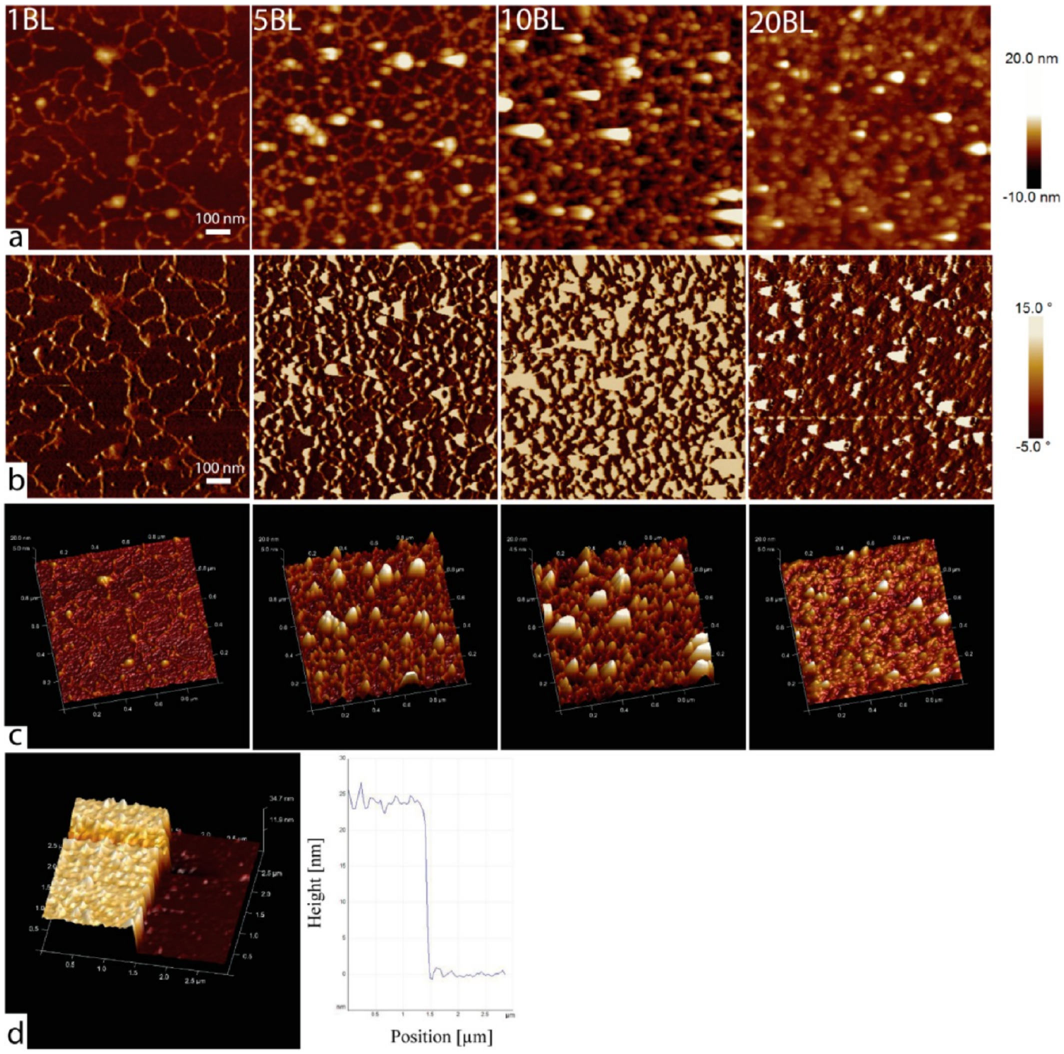

Figure 3. AFM tapping mode: (a) height, (b) phase, (c) 3D morphology images of (CH/PVPA) on silica substrates with increasing number of bilayers (left to right 1, 5, 10, and 20 BL), and (d) height profiles of a scratched 20 BL thin film. The images are 1 × 1 μm and the z-range is indicated in the scale bar to the right in the figures.

results.[57] The thickness measurement on the scratched film shows that the thickness of 20 BL film was 25 nm.

Adsorption of CH and PVPA onto Cellulose Fibers Using Polyelectrolyte Titration. Chitosan and poly(vinylphosphonic acid) are both weak polyelectrolytes with charge densities that are pH-dependent. The charge densities of the polyelectrolytes were determined by polyelectrolyte titration (PET) using KPVS for CH and PDADMAC for PVPA, and the values obtained were utilized to establish the adsorption isotherm for the chitosan in the first layer (Supporting Information, Figure S1) and the total adsorbed amounts of PVPA and CH in the following layers. The adsorption isotherm for the CH reached a plateau at 2.6 mg chitosan/g fiber. We therefore used 10 mg CH/g fiber to ensure a recharging of the fibers in the LbL treatment and 10 mg/g of the PVPA was used for the anionic layer. The amount of polymer adsorbed in each layer was then determined by polyelectrolyte titration of the nonadsorbed polymer in the residual solution after the adsorption, as shown in Figure 4. After 20 BL, the adsorbed amount was 61 mg/g of CH and 97 mg/g of PVPA, and this follows the trend detected in the QCM-D measurements.

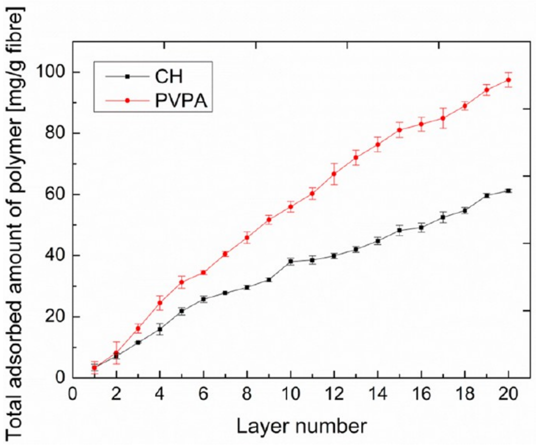

Figure 4. Cumulative adsorbed amount of CH and PVPA onto cellulose fibers as a function of layer number determined by polyelectrolyte titration. The pH was kept constant at 4, and the salt concentration was 10 mM NaCl.

Thermal Stability of Fibers. The thermal and thermo-oxidative stability of the cellulose fibers and the LbL-coated

(CH/PVPA) cellulose fibers were investigated by thermogravimetric analysis under both nitrogen and air. The data are summarized in Table 1, and Figure 5 shows weight loss and derivative curves in (a) nitrogen and (b) air. From earlier investigations,[58] it was expected that the cellulose pyrolysis would proceed in one step under nitrogen. The degradation of the uncoated reference fibers occurs around 350 °C and is the result of two competitive pathways: the depolymerization of glycosyl units into volatile products (levoglucosan) and the decomposition of the same units to thermally stable aromatic char (residue). The degradation of the multilayer-treated fibers also occurred in a single step, but the weight of the residue at the end of the degradation increased significantly with 10 and 20 BL, as shown in Table 1.

Table 1. TGA Data of Pure and CH/PVPA-Treated Paper under Nitrogen and Air

sample	$T_{\text{onset }10\%}$ (°C)	$T_{\max1}$ (°C)[a]	$T_{\max2}$ (°C)[a]	residue at 600 °C (%)
nitrogen paper	323	365		13
1BL CH/PVPA	332	365		13
5BL CH/PVPA	332	371		13
10BL CH/PVPA	329	354		20
20BL CH/PVPA	328	350		25
air paper	310	341	471	1
1BL CH/PVPA	316	341	476	1
5BL CH/PVPA	317	341	503	2
10BL CH/PVPA	314	332	508	6
20BL CH/PVPA	318	332	521	9

[a] From derivative weight loss curves.

In air, the thermal oxidation of cellulose occurred in two steps.[59] The first step between 300 and 400 °C is due to formation of both volatiles and aliphatic char, and this latter substance is further oxidized during the second degradation step (400–600 °C) to produce both CO and CO_2. As in the case of nitrogen, untreated and treated fibers show a similar degradation pattern, but the residue produced after the first degradation step increased with increasing BL number to 10 and 20, while the second degradation step was shifted toward higher temperatures, as shown by the $T_{\max2}$ values in Table 1. The final residue at 600 °C increased in proportion to BL number.

Flame-Retardant Behavior. Sheets prepared from untreated and LbL-treated wood fibers were subjected to horizontal flame testing. This test evaluates the propensity of a material to propagate fire when exposed to a small flame. Table 2 shows the results, and Figure 6 shows photographs of

Table 2. Flammability Data for Untreated and CH/PVPA-Treated Paper

sample	burning time (s)	after-glow time (s)	burning rate (mm/s)	residue (%)
control	60 ± 6	5 ± 1	1.5 ± 0.1	
1BL	57 ± 2	7 ± 2	1.6 ± 0.1	
5BL	52 ± 2		1.9 ± 0.1	9
10BL	53 ± 5		1.9 ± 0.2	11
20BL	38 ± 8		1.7 ± 0.1	70

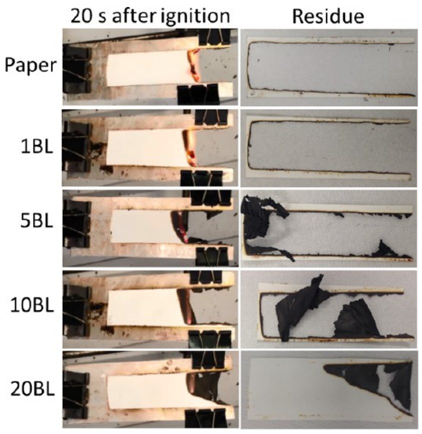

Figure 6. Photographs taken 20 s after ignition with a methane torch of untreated and CH/PVPA LbL-treated paper and of the residues at the end of the horizontal flame test. The numbers to the left show the number of bilayers added to the fibers before sheet preparation.

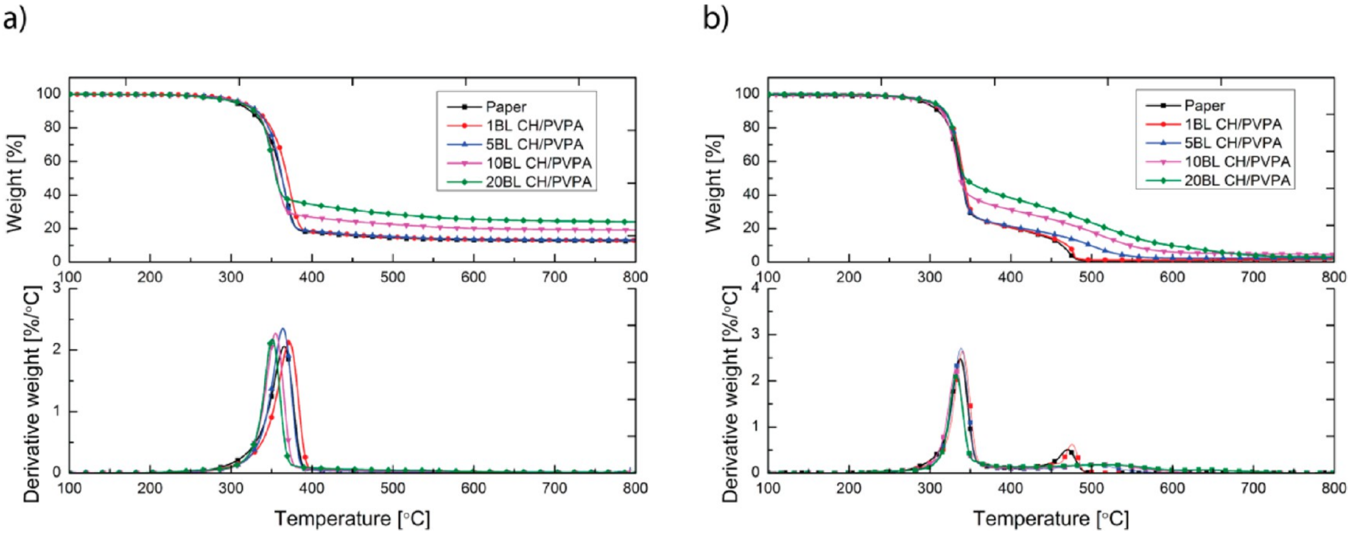

Figure 5. Weight loss and derivative weight loss plots of untreated and CH/PVPA-treated paper measured under (a) nitrogen and (b) air atmospheres.

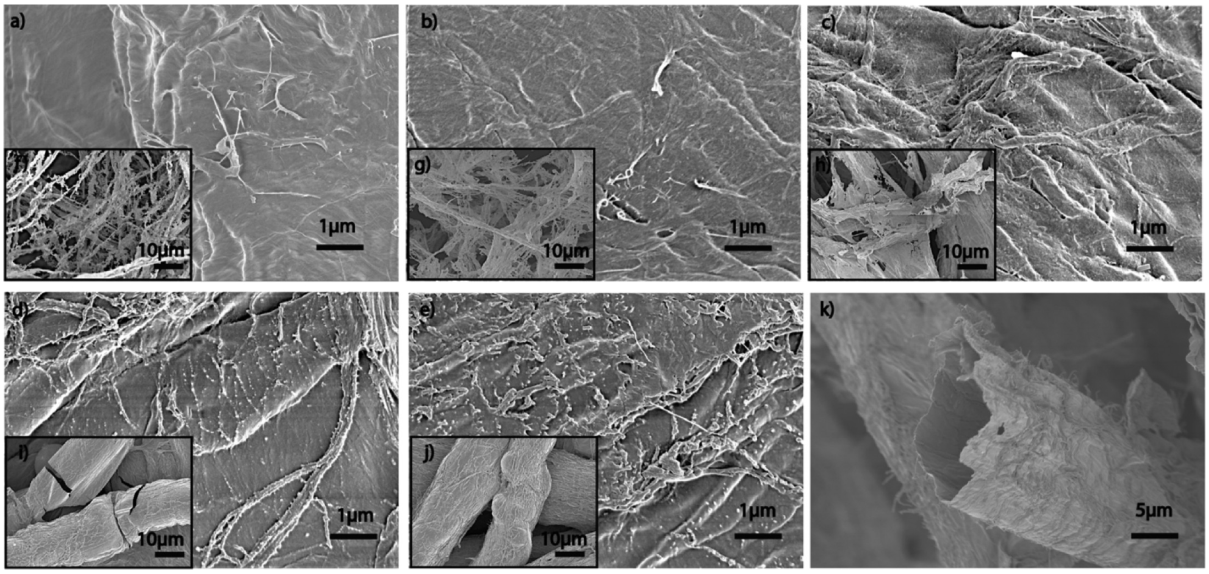

Figure 7. SEM images of fibers before and after LbL treatment and before and after horizontal flame test; (a) control and coated with CH/PVPA (b) 1BL, (c) 5BL, (d) 10BL, and (e) 20BL. SEM images of pulp fibers after horizontal flame test, (f) control, (g) 1BL, (h) 5BL, (i) 10BL, (j) 20BL, and (k) cross section of 20BL.

the tests on the different samples. When exposed to a direct methane flame untreated paper sheets immediately ignite and burn completely in less than 1 min, leaving no residue. After the flame was extinguished, the afterglow combustion completely consumed the residue. Afterglow is considered dangerous because, even without a flame, the high temperatures reached can still spread the fire. LbL-treated wood fibers show a significant reduction in the total burning time and a larger amount of coherent residue at the end of the test. There was no afterglow in the case of the CH/PVPA at 5, 10, and 20 BL. The 20 BL samples showed a self-extinguishing behavior, with the advancing flame was gradually restricted to a smaller portion of the sample showing a reduction in size and spread rate and eventually vanishing (Figure 6). As a consequence, the final residue left at the end of the test was as high as 70%.

Morphological Analysis. Scanning electron microscopy (SEM) was employed to investigate the surface morphology and structure of the fibers before and after treatment of the CH/PVPA LbL-assembly. The SEM micrographs of untreated, 1, 5, 10, and 20 BL of CH/PVPA-coated fibers are shown in Figure 7a-e. The change in the surface morphology of the fibers due to polyelectrolyte adsorption is shown in the high magnification SEM images. Fibril-like aggregates on the fiber surface at higher BL numbers clearly demonstrate the deposition of the polyelectrolyte thin film. The size of the aggregates and their surface coverage increase become more visible with increasing BL number. Fractured fibers were investigated in order to clarify structure of deposited layers and fiber−fiber interactions after LbL treatment (Supporting Information, Figure S2). The residues after the flammability tests were also examined by SEM in order to see whether the treatment had resulted in any significant changes. Untreated sample burned completely leaving a small ash residue (Figure 7f), and the dimensional and structural losses caused by combustion are gradually prevented by increasing the BL number. The best protection is observed with fibers containing 20 BL and, as shown in Figure 7j,k, these fibers preserve their original texture and shape. Cross-section imaging of the residue of the 20BL samples (Figure 7k) demonstrates a remarkably preserved structure of the BL coating, showing hollow fibers where basically all the cellulose is removed.

Cone Calorimetry. Cone calorimetry was used to evaluate the sheets prepared from LbL-treated pulp fibers because it can show quantitative differences between differently treated fibers. Thus, the combustion behavior of the samples was evaluated using cone calorimetry under an irradiating heat flux of 35 kW/m^2, which is typically found during fire development. As a consequence of the high temperature reached under the cone, the sample starts degrading, releasing combustible volatile gases that, after a certain time, lead to ignition and flaming combustion. The time to ignition (TTI, s), total heat release (THR, MJ/m^2), peak heat release rate (pkHRR, kW/m^2) and residue (%) are summarized in Table 3. The combustion of the paper sheet is clearly influenced by the presence of the polyelectrolyte thin film. The pkHRR was gradually reduced by increasing the BL number. The final residues collected at the end of the test followed a similar trend. The fire growth rate index (FIGRA) has been introduced as an indication of the burning tendency of a material exposed to heat. FIGRA is the peak heat release rate divided by the time to reach to peak heat release rate (pkHRR). It is shown in Table 3 that CH/PVPA 20 BL coatings can reduce the FIGRA value by up to 38%. Additional cone calorimetry tests data concerning the weight of the samples before the test can be found in the Supporting Information (Table S1).

Table 3. Cone Calorimetry Data for Pure Paper and Paper Prepared with (CH/PVPA)-Treated Pulp

sample	TTI (s)	THR (MJ/m^2)	pkHRR (kW/m^2)	FIGRA (kW/sm^2)	residue (%)
control	38 ± 7	1.2 ± 0.2	83 ± 5	2.1 ± 0.4	
1BL	32 ± 4	1.2 ± 0.3	76 ± 3	2.1 ± 0.2	1 ± 1
5BL	37 ± 5	0.8 ± 0.3	65 ± 11	1.7 ± 0.5	6 ± 1
10BL	39 ± 3	0.6 ± 0.3	59 ± 14	1.4 ± 0.3	9 ± 2
20BL	32 ± 12	0.8 ± 0.2	42 ± 7	1.3 ± 0.6	12 ± 1

DISCUSSION

Multilayer Film Characterization. The buildup of CH/PVPA bilayers on the pulp fibers have been investigated using a combination of QCM-D measurements with model cellulose surfaces and adsorption studies on fibers using polyelectrolyte titration. The results show the same trends, so that the QCM-D measurements can be used to forecast the properties of the layers formed on the fibers. The results in Figure 2 show that there is a steady buildup of the layers both under salt free conditions and in 10 mM NaCl. On the other hand, the decrease in frequency was much higher with 10 mM NaCl than without salt, indicating a larger adsorbed mass at the higher ionic strength, and suggesting that polymer chains are more densely packed on the surface. The energy dissipation increases with the adsorption of CH and decreases with rinsing which is probably due to the formation of a more compact and rigid layer due to a relaxation or reconformation of CH chains toward the interface during the washing stage, since the change in frequency is small during the rinsing stage. The change in energy dissipation is smaller for LbL assembly in 10 mM NaCl, which implies that the CH and PVPA layers are more firmly and densely attached to the underlying surface at this salt concentration. Furthermore, the change in frequency is essentially independent of the number of the overtone throughout the assembly, which suggests that the structure of the films is the same at a given distance from the solid substrate. The Sauerbrey relation can be used to estimate the adsorbed mass from the observed frequency shift even though care must be taken not to overinterpret the collected data considering the measuring principle.[60] Figure 2d shows the adsorbed amount of polyelectrolyte including associated solvent. It is also possible to compare the buildup of the LbL on SiO_2 surfaces using ellipsometry (i.e., showing only the solid adsorbed amount) with the adsorption given by the QCM-D giving both the solid adsorbed amount and the immobilized liquid in the adsorbed layer. Assuming that the buildup of the layers is similar on both types of surfaces, this comparison indicates that the amount of water associated with the adsorption is lower in the more external layer because adsorption shows a constant increase with increasing layer number in QCM-D, but a more superlinear development according to the ellipsometry measurements. By combining these results with the results from the AFM measurements, it can be suggested that it is necessary to deposit a number of BLs between 5 and 10 to obtain a film formation on the surface. This is in agreement with recently published results using chitosan and poly(sodiumphosphate) for the LbL formation.[55] Once this film formation has been achieved, the films become smoother with increasing layer number and there is a very close correlation between the results of ellipsometry measurements and the AFM measurements showing the formation of a 20−25 nm thick, dry LbL film with 20 BLs. Assuming a density in the adsorbed layer of 1×10^3 kg/m^3, the average solids content of the 20 BL film is 50%, which is a rather dense LbL film. All these results taken together mean that in order to form a film of CH/PVPA on the fibers, more than 10 BLs have to be adsorbed and with 20 BLs, a 25 nm thick film is achieved. In addition, SEM observations performed on the cross section of 20BL samples demonstrated that, despite the heterogeneity of fiber fracture, the fiber−fiber interaction was not affected by the LbL coating.

Thermal Stability and Flame-Retardant Properties. All CH/PVPA-coated pulp fibers show an initial degradation temperature similar to that of the unmodified fibers. However, (CH/PVPA) LbL-treated fibers exhibit an increased char forming ability as demonstrated by the residue found in the range of 400−600 °C, that significantly increases with increasing number of deposited BLs. This can certainly be ascribed to the presence of the LbL coating, where the PVPA can act as a phosphoric acid source favoring char formation from chitosan and creating a protective char layer on the surface of each treated fiber. With the protective layer generated by the LbL-coating, the degradation of cellulose fibers is retarded and the formation of char is favored.[12,15,37,59] The same mechanism was demonstrated during flammability tests and, the char barrier generated by the coating is capable of retarding the heat and mass transfer between the flame and the fibers. This effect increases with increasing number of deposited BLs, and 20 BLs are sufficient to decrease the release of volatile species and provide heat shielding leading to a self-extinguishing behavior. This excellent result is linked to the good surface coverage achieved with the LbL coatings, as demonstrated by the model adsorption studies and by the SEM micrographs (Figure 7c−e). SEM micrographs of the paper sheets after the flame test (Figure 7f−j) show that the fibers retain their structure as a result of the flame-retardant behaviors. Interestingly, the protective char layer did not show the traditional bubbles observed in intumescent flame-retardant systems, which can be ascribed to the low thickness of the LbL assemblies (25 nm at 20 BL) due to the high charge densities of the polyelectrolytes in the deposition conditions adopted.[59] Moreover, hollow fibers were found (Figure 7k) in the 20 BL CH/PVPA-treated pulp fibers, indicating the formation of coherent and intact charred layer on the fiber wall. The amount of CH adsorbed, 61 mg/g fiber and of PVPA 97 mg/g fiber (20 bilayers), was sufficient to impart self-extinguishing properties to the paper sheet (Figure 4b).

By cone calorimetry the char-forming ability of the LbL coating has been found responsible for a decrease in the pkHRR value proportional to the number of deposited BL (i.e., an increase in the BL number lowers the combustion rate of cellulosic materials). It is important to note that the incorporation of CH/PVPA did not change the TTI value of paper sheets. This was also supported by TGA measurements, where an increase in the number of deposited bilayers did not alter the degradation temperature (T_{onset}) of cellulose. Such a finding is interesting because one of the peculiar characteristics of intumescent systems deposited by LbL is that the time to ignition under cone calorimetry is reduced. This detrimental reduction has been explained by the presence of a strong acid. No reduction in TTI in the CH/PVPA system can thus be considered positive and may be related to the particular structure of these LbL assemblies. This is also reflected with decrease in the FIGRA values with increasing number of BL, revealing the suppression of the possible flame spread.

CONCLUSIONS

A novel approach for the production of flame-retardant paper via layer-by-layer assembly has been presented. LbL assemblies of CH and PVPA have been thoroughly characterized through model studies, using both cellulose and SiO_2, and have been successfully formed on wood-based fibers. The addition of 10 mM NaCl as background electrolyte increased the total adsorbed amount of polymer, and the pH was kept constant at 4 to ensure good solubility of the chitosan. The thin film surface coverage improved as a function of the number of bilayers, and to achieve full surface coverage, it was necessary to form between 5 and 10 BL. At 20 BL, the film reached a dry thickness of 25 nm. By comparing ellipsometry and QCM-D measurements the solids content of the formed film was found to be around 50% for 20 BLs. Thermogravimetric analysis revealed an increase in the char-forming ability of treated fibers compared with uncoated ones. During the horizontal flame tests, the flame self-extinguished on a paper sheet coated with 20 bilayers of CH/PVPA due to the formation of a coherent and intact char layer on the fibers. After the flammability test, the treated wood fibers retained their shape and structure, while the unmodified fibers were completely destroyed, as shown in SEM images. Cone calorimetry revealed a strong reduction in the peak heat release rate with increasing number of deposited BL, reaching the best performances at 20 BL. The application of 20 bilayers will naturally be difficult in large scale paper production but probably a similar flame-retardant effect can be achieved with considerably fewer numbers of bilayers. Furthermore, we are currently evaluating different addition strategies to achieve similar results with fewer treatment steps, and at the same time, Pettersson et al. showed where the LbL technology can indeed be used in pilot scale paper production without any major difficulties.[61] All the above considerations make this LbL CH/PVPA nanocoating an effective and environmentally benign flame-retardant system for wood-fiber-based paper sheets.

■ ASSOCIATED CONTENT

Ⓢ Supporting Information

The Supporting Information is available free of charge on the ACS Publications website at DOI: 10.1021/acsami.5b08105.

> Adsorption saturation level of chitosan from the adsorption isotherm obtained by polyelectrolyte titration, cone calorimetry experimental data, and scanning electron microscopy images of fractured fibers. (PDF)

■ AUTHOR INFORMATION

Corresponding Authors

*Email: oruc@kth.se.
*Email: wagberg@kth.se.

Author Contributions

The manuscript was written through contributions of all authors. All authors have given approval to the final version of the manuscript.

Notes

The authors declare no competing financial interest.

■ ACKNOWLEDGMENTS

L.W., O.K., and F.C. acknowledge financial support from SSF (The Foundation for Strategic Research). L.W. also acknowledges The Wallenberg Wood Science Centre for financial support. Dr. Mats Sandberg, Acreo AB, Norrköping, Sweden is also thanked for supporting us with a sample of poly(-vinylphosphonic acid).

■ REFERENCES

(1) Ek, M.; Gellerstedt, G.; Henriksson, G. *Volume 1 Wood Chemistry and Wood Biotechnology* **2009**.

(2) Whitehead, J. B.; Greenfield, E. W. Dielectric Properties of Cellulose Paper-I. *Electr. Eng.* **1934**, *53*, 1389−1396.

(3) Horrocks, A. R. Developments in flame retardants for heat and fire resistant textiles—the role of char formation and intumescence. *Polym. Degrad. Stab.* **1996**, *54*, 143−154.

(4) FIRE RETARDANT PAPER AND PAPER BOARD. US Patent 3,770,577: 1973.

(5) Katović, D.; Vukušić, S.; Grgac, S.; Lozo, B.; Banić, D. Flame retardancy of paper obtained with environmentally friendly agents. *Nucl. Med. Rev. Cent East Eur.* **2009**, *17*, 90−94.

(6) Nassar, M. M.; Fadali, O. A.; Khattab, M. A.; Ashour, E. A. Thermal studies on paper treated with flame−retardant. *Fire Mater.* **1999**, *23*, 125−129.

(7) de Wit, C. A. An overview of brominated flame retardants in the environment. *Chemosphere* **2002**, *46*, 583−624.

(8) Stieger, G.; Scheringer, M.; Ng, C. A.; Hungerbühler, K. Assessing the persistence, bioaccumulation potential and toxicity of brominated flame retardants: Data availability and quality for 36 alternative brominated flame retardants. *Chemosphere* **2014**, *116*, 118−123.

(9) Malucelli, G.; Carosio, F.; Alongi, J.; Fina, A.; Frache, A.; Camino, G. Materials engineering for surface-confined flame retardancy. *Mater. Sci. Eng., R* **2014**, *84*, 1−20.

(10) Li, Y.-C.; Schulz, J.; Grunlan, J. C. Polyelectrolyte/nanosilicate thin-film assemblies: influence of pH on growth, mechanical behavior, and flammability. *ACS Appl. Mater. Interfaces* **2009**, *1*, 2338−2347.

(11) Li, Y.-C.; Schulz, J.; Mannen, S.; Delhom, C.; Condon, B.; Chang, S.; Zammarano, M.; Grunlan, J. C. Flame retardant behavior of polyelectrolyte− clay thin film assemblies on cotton fabric. *ACS Nano* **2010**, *4*, 3325−3337.

(12) Laufer, G.; Kirkland, C.; Cain, A. A.; Grunlan, J. C. Clay−chitosan nanobrick walls: completely renewable gas barrier and flame-retardant nanocoatings. *ACS Appl. Mater. Interfaces* **2012**, *4*, 1643−1649.

(13) Apaydin, K.; Laachachi, A.; Ball, V.; Jimenez, M.; Bourbigot, S.; Toniazzo, V.; Ruch, D. Polyallylamine−montmorillonite as super flame retardant coating assemblies by layer-by layer deposition on polyamide. *Polym. Degrad. Stab.* **2013**, *98*, 627−634.

(14) Alongi, J.; Di Blasio, A.; Carosio, F.; Malucelli, G. UV-cured hybrid organic−inorganic Layer by Layer assemblies: Effect on the flame retardancy of polycarbonate films. *Polym. Degrad. Stab.* **2014**, *107*, 74−81.

(15) Carosio, F.; Alongi, J.; Malucelli, G. Layer by Layer ammonium polyphosphate-based coatings for flame retardancy of polyester−cotton blends. *Carbohydr. Polym.* **2012**, *88*, 1460−1469.

(16) Carosio, F.; Laufer, G.; Alongi, J.; Camino, G.; Grunlan, J. C. Layer-by-layer assembly of silica-based flame retardant thin film on PET fabric. *Polym. Degrad. Stab.* **2011**, *96*, 745−750.

(17) Iler, R. Multilayers of colloidal particles. *J. Colloid Interface Sci.* **1966**, *21*, 569−594.

(18) Decher, G.; Hong, J. D. In Buildup of ultrathin multilayer films by a self−assembly process, 1 consecutive adsorption of anionic and cationic bipolar amphiphiles on charged surfaces, *Makromolekulare Chemie. Macromolecular Symposia*; Wiley Online Library: 1991; pp 321−327.

(19) Hammond, P. T. Form and function in multilayer assembly: new applications at the nanoscale. *Adv. Mater.* **2004**, *16*, 1271−1293.

(20) Berndt, P.; Kurihara, K.; Kunitake, T. Adsorption of poly(styrenesulfonate) onto an ammonium monolayer on mica: a surface forces study. *Langmuir* **1992**, *8*, 2486−2490.

(21) Shimazaki, Y.; Mitsuishi, M.; Ito, S.; Yamamoto, M. Preparation of the Layer-by-Layer Deposited Ultrathin Film Based on the Charge-Transfer Interaction. *Langmuir* **1997**, *13*, 1385−1387.

(22) Bergbreiter, D. E.; Tao, G.; Franchina, J. G.; Sussman, L. Polyvalent Hydrogen-Bonding Functionalization of Ultrathin Hyper-branched Films on Polyethylene and Gold. *Macromolecules* **2001**, *34*, 3018−3023.

(23) Sun, J.; Wu, T.; Liu, F.; Wang, Z.; Zhang, X.; Shen, J. Covalently Attached Multilayer Assemblies by Sequential Adsorption of Polycationic Diazo-Resins and Polyanionic Poly(acrylic acid). *Langmuir* **2000**, *16*, 4620−4624.

(24) Jang, W.-S.; Grunlan, J. C. Robotic dipping system for layer-by-layer assembly of multifunctional thin films. *Rev. Sci. Instrum.* **2005**, *76*, 103904.
(25) Schlenoff, J. B.; Dubas, S. T.; Farhat, T. Sprayed polyelectrolyte multilayers. *Langmuir* **2000**, *16*, 9968−9969.
(26) Mermut, O.; Barrett, C. J. Effects of charge density and counterions on the assembly of polyelectrolyte multilayers. *J. Phys. Chem. B* **2003**, *107*, 2525−2530.
(27) Sui, Z.; Salloum, D.; Schlenoff, J. B. Effect of molecular weight on the construction of polyelectrolyte multilayers: stripping versus sticking. *Langmuir* **2003**, *19*, 2491−2495.
(28) Tan, H. L.; McMurdo, M. J.; Pan, G.; Van Patten, P. G. Temperature dependence of polyelectrolyte multilayer assembly. *Langmuir* **2003**, *19*, 9311−9314.
(29) Zhang, H.; Rühe, J. Interaction of strong polyelectrolytes with surface-attached polyelectrolyte brushes-polymer brushes as substrates for the layer-by-layer deposition of polyelectrolytes. *Macromolecules* **2003**, *36*, 6593−6598.
(30) McAloney, R. A.; Sinyor, M.; Dudnik, V.; Goh, M. C. Atomic force microscopy studies of salt effects on polyelectrolyte multilayer film morphology. *Langmuir* **2001**, *17*, 6655−6663.
(31) Shiratori, S. S.; Rubner, M. F. pH-dependent thickness behavior of sequentially adsorbed layers of weak polyelectrolytes. *Macromolecules* **2000**, *33*, 4213−4219.
(32) Priolo, M. A.; Gamboa, D.; Holder, K. M.; Grunlan, J. C. Super gas barrier of transparent polymer− clay multilayer ultrathin films. *Nano Lett.* **2010**, *10*, 4970−4974.
(33) Li, Z.; Lee, D.; Sheng, X.; Cohen, R. E.; Rubner, M. F. Two-level antibacterial coating with both release-killing and contact-killing capabilities. *Langmuir* **2006**, *22*, 9820−9823.
(34) Hiller, J. A.; Mendelsohn, J. D.; Rubner, M. F. Reversibly erasable nanoporous anti-reflection coatings from polyelectrolyte multilayers. *Nat. Mater.* **2002**, *1*, 59−63.
(35) Shim, B. S.; Tang, Z.; Morabito, M. P.; Agarwal, A.; Hong, H.; Kotov, N. A. Integration of conductivity, transparency, and mechanical strength into highly homogeneous layer-by-layer composites of single-walled carbon nanotubes for optoelectronics. *Chem. Mater.* **2007**, *19*, 5467−5474.
(36) Camino, G.; Costa, L.; Martinasso, G. Intumescent fire-retardant systems. *Polym. Degrad. Stab.* **1989**, *23*, 359−376.
(37) Li, Y. C.; Mannen, S.; Morgan, A. B.; Chang, S.; Yang, Y. H.; Condon, B.; Grunlan, J. C. Intumescent All−Polymer Multilayer Nanocoating Capable of Extinguishing Flame on Fabric. *Adv. Mater.* **2011**, *23*, 3926−3931.
(38) Laufer, G.; Kirkland, C.; Morgan, A. B.; Grunlan, J. C. Intumescent multilayer nanocoating, made with renewable polyelectrolytes, for flame-retardant cotton. *Biomacromolecules* **2012**, *13*, 2843−2848.
(39) Agarwal, M.; Lvov, Y.; Varahramyan, K. Conductive wood microfibres for smart paper through layer-by-layer nanocoating. *Nanotechnology* **2006**, *17*, 5319.
(40) Wagberg, L.; Forsberg, S.; Johansson, A.; Juntti, P. Engineering of fibre surface properties by application of the polyelectrolyte multilayer concept. Part I: Modification of paper strength. *J. Pulp Pap. Sci.* **2002**, *28*, 222−228.
(41) Gustafsson, E.; Larsson, P. A.; Wågberg, L. Treatment of cellulose fibres with polyelectrolytes and wax colloids to create tailored highly hydrophobic fibrous networks. *Colloids Surf., A* **2012**, *414*, 415−421.
(42) Eriksson, M.; Notley, S. M.; Wågberg, L. The influence on paper strength properties when building multilayers of weak polyelectrolytes onto wood fibres. *J. Colloid Interface Sci.* **2005**, *292*, 38−45.
(43) Lingström, R.; Wågberg, L. Polyelectrolyte multilayers on wood fibers: Influence of molecular weight on layer properties and mechanical properties of papers from treated fibers. *J. Colloid Interface Sci.* **2008**, *328*, 233−242.
(44) Srikulkit, K.; Iamsamai, C.; Dubas, S. T. Development of flame retardant polyphosphoric acid coating based on the polyelectrolyte multilayers technique. *J. Met., Mater. Miner.* **2006**, *16*, 41−45.
(45) Wang, L.-l.; Zhang, T.; Yan, H.-q.; Fang, Z.-p.; Li, Y.; Hao, W.; Peng, M. Flame-retardant coating by alternate assembly of poly (vinylphosphonic acid) and polyethylenimine for ramie fabrics. *Chin. J. Polym. Sci.* **2014**, *32*, 305−314.
(46) Wågberg, L.; Hägglund, R. Kinetics of Polyelectrolyte Adsorption on Cellulosic Fibers. *Langmuir* **2001**, *17*, 1096−1103.
(47) Wagberg, L.; Odberg, L.; Glad-Nordmark, G. Charge determination of porous substrates by polyelectrolyte adsorption Part 1. Carboxymethylated, bleached cellulosic fibers. *Nord. Pulp Pap. Res. J.* **1989**, *4*, 071−076.
(48) Swerin, A.; Wågberg, L. Size-exclusion chromatography for characterization of cationic polyelectrolytes used in papermaking. *Nord. Pulp Pap. Res. J.* **1994**, *9*, 18−25.
(49) Gunnars, S.; Wågberg, L.; Cohen Stuart, M. A. Model films of cellulose: I. Method development and initial results. *Cellulose* **2002**, *9*, 239−249.
(50) Enarsson, L.-E.; Wågberg, L. Polyelectrolyte Adsorption on Thin Cellulose Films Studied with Reflectometry and Quartz Crystal Microgravimetry with Dissipation. *Biomacromolecules* **2008**, *10*, 134−141.
(51) Rodahl, M.; Höök, F.; Krozer, A.; Brzezinski, P.; Kasemo, B. Quartz crystal microbalance setup for frequency and Q−factor measurements in gaseous and liquid environments. *Rev. Sci. Instrum.* **1995**, *66*, 3924−3930.
(52) Sauerbrey, G. Verwendung von Schwingquarzen zur Wägung dünner Schichten und zur Mikrowägung. *Eur. Phys. J. A* **1959**, *155*, 206−222.
(53) Terayama, H. Method of colloid titration (a new titration between polymer ions). *J. Polym. Sci.* **1952**, *8*, 243−253.
(54) Tata, J.; Alongi, J.; Carosio, F.; Frache, A. Optimization of the procedure to burn textile fabrics by cone calorimeter: part I. Combustion behavior of polyester. *Fire Mater.* **2011**, *35*, 397−409.
(55) Mateos, A. J.; Cain, A. A.; Grunlan, J. C. Large-Scale Continuous Immersion System for Layer-by-Layer Deposition of Flame Retardant and Conductive Nanocoatings on Fabric. *Ind. Eng. Chem. Res.* **2014**, *53*, 6409−6416.
(56) Notley, S. M.; Eriksson, M.; Wågberg, L. Visco-elastic and adhesive properties of adsorbed polyelectrolyte multilayers determined in situ with QCM-D and AFM measurements. *J. Colloid Interface Sci.* **2005**, *292*, 29−37.
(57) Apaydin, K.; Laachachi, A.; Ball, V.; Jimenez, M.; Bourbigot, S.; Toniazzo, V.; Ruch, D. Intumescent coating of (polyallylamine-polyphosphates) deposited on polyamide fabrics via layer-by-layer technique. *Polym. Degrad. Stab.* **2014**, *106*, 158−164.
(58) Alongi, J.; Camino, G.; Malucelli, G. Heating rate effect on char yield from cotton, poly (ethylene terephthalate) and blend fabrics. *Carbohydr. Polym.* **2013**, *92*, 1327−1334.
(59) Carosio, F.; Negrell-Guirao, C.; Di Blasio, A.; Alongi, J.; David, G.; Camino, G. Tunable thermal and flame response of phosphonated oligoallylamines layer by layer assemblies on cotton. *Carbohydr. Polym.* **2015**, *115*, 752−759.
(60) Boulmedais, F.; Ball, V.; Schwinte, P.; Frisch, B.; Schaaf, P.; Voegel, J.-C. Buildup of Exponentially Growing Multilayer Polypeptide Films with Internal Secondary Structure. *Langmuir* **2003**, *19*, 440−445.
(61) Pettersson, G.; Höglund, H.; Norgren, S.; Sjöberg, J.; Peng, F.; Hallgren, H.; Moberg, A.; Ljungqvist, C.-H.; Bergström, J.; Solberg, D. Strong and bulky paperboard sheets from surface modified CTMP, manufactured at low energy. *Nord. Pulp Pap. Res. J.* **2015**, *30*, 318−324.